IJST (2013) 37A2: 147-159
Iranian Journal of Science & Technology

http://www.shirazu.ac.ir/en

Geochemical characterization and petrogenesis of Niat-Jal amphibolites, southeast Kohistan, Pakistan

M. Ahmed Khan[1], S. U. Rehman*[2], K. Mehmood[2], M. Asif Khan[3] and N. Ahsan[4]

Continental Laboratories Ltd.3601-A, 21st Street NE, Calgary, Canada
Department of Earth Sciences, University of Sargodha, Sargodha, 41000, Pakistan
NCE Geology, Peshawar University, Peshawar, Pakistan
Institute of Geology, University of Punjab, Lahore
E-mail: saif.rehman@uos.edu.pk

Abstract

The Kamila Amphibolite Unit (KAU) of southeast Kohistan, Pakistan, represents a thick sequence of meta-volcanics which is underlined by the mafic-ultramafic rocks of the Spat Complex along the MMT (Main Mantle Thrust). The meta-volcanics of KAU are intruded by diorites, granitoids and tronjhemites of the Thak intusive complex. KAU is subdivided into four distinct units; Babusar, Niat and Jal amphibolites from south to north with a thin slice of Sumal amphibolites within Niat-Jal amphibolites. Niat and Jal amphibolites generally show strong foliation and alternating bands of mafic and felsic compositions. Niat amphibolites are generally fine to medium grained and composed of amphibole (hornblende and actinolite) and substantial quartz with subordinate plagioclase, epidote and chlorite. Magnetite, sphene, muscovite, and apatite occur as accessory minerals. The Jal amphibolites are fine grained and melanocratic and generally comprised of hornblende and plagioclase with subordinate quartz and sericite. Epidote and sphene occur as accessory minerals. Twenty six samples from both groups have been analyzed for whole rock geochemistry. The studied amphibolites fall in tholeiite group and show enrichment in HFS elements and depletion in LIL elements. Spider diagrams and MgO versus Zr plot show heterogeneous compositional patterns, with three distinct patterns: primitive, less evolved and more evolved. Average concentration of TiO2 (1.99 wt% for Niat amphibolites and 1.56 wt% for Jal amphibolites) and K2O (0.14 wt% for Niat amphibolites and 0.20 wt% for Jal amphibolites) exhibit MORB like composition whereas average Y/Nb ratio (8.9 for Niat amphibolites and 8.4 for Jal amphibolites) are close to N-MORB. Zr/Y vs Zr plot characterized the studied rocks as MORB and they fall in the ocean floor basalt (OFB) field on the triangular Ti/100, Zr, Y*3 diagram.

***Keywords**:* Kohistan island arc; Kamila amphibolites unit; Niat aphibolites; Jal amphibolites

1. Introduction

The intra-oceanic Kohistan island arc was initiated during the Cretaceous as a result of northward movement of the Indian Plate [1] and was sandwiched between the Indian and Eurasian plates (Fig. 1) [2, 3]. It constitutes a territory of about 36000 square kilometers. The Kohistan sequence represents rocks of a young arc crust comprising amphibolites, diorites, metanorites and associated volcanic rocks [4]. Amphibolites are prominently found along the southern belt of the Kohistan sequence [5] which extends from Afghanistan through Bajaur, Dir, Swat, Indus Valley, Babusar [6,7,8], up to Nanga Parbat [9].

The Kamila amphibolite unit [10, 11], a strip (maximum 50×50 km) of amphibolites, constitutes the southeastern part of Kohistan (Fig. 1 & 2). [12] and [13] included this unit in their “Upper Swat Hornblendic group”. The name “Kohistan Basic Complex” was used by [14] for basic rocks of southern Kohistan. Various investigators [15, 16] introduced the name “Kamila amphibolite belt”, whereas others [5, 17-20] refer to these amphibolites as “Southern amphibolites”.

The Kamila amphibolite unit is confined between the Main Mantle Thrust [4] in the south and Chilas Complex in the north along Jal shear zone, in the southern part of the Kohistan terrain [15, 18]. The unit is distinguished by mafic-ultramafics rocks of Sapat Complex [21, 22] at the base from MMT (Fig. 2). The Sapat complex is composed of a variety of lithologies including dunite, pyroxenites, peridotites, chromitite, gabbros and anorthosite [22, 23]. Ultramafic rocks generally occur as lensoid bodies within layered and isotropic gabbroic rocks [10]. The Kamila amphibolite unit is divisible into three linear belts; Babusar amphibolites, Niat and Jal amphibolites from south to north, and a thin

*Corresponding author
Received: 20 December 2011 / Accepted: 16 October 2012

slice within Niat and Jal amphibolites named Sumal amphibolites [3, 10, 11]. Amphibolites are intruded by diorites/tonalite, granodiorites, trondhjemites, granites and some gabbro of the Thak intrusive complex. These rocks occur as sheet like lenticular masses and minor intrusives in the form of veins, sills or dykes [3, 10, 11, 24, and 25]. This paper is aimed to present the integrated summary of the Jal-Niat amphibolites of the kamila Amphibolite Unit to elucidate their petrography, petrogenesis and tectonic environments.

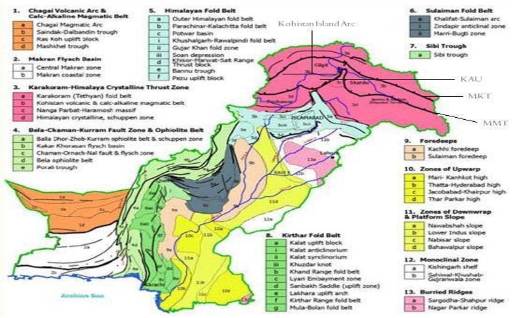

Fig. 1. Tectonic map of Pakistan (after [2])

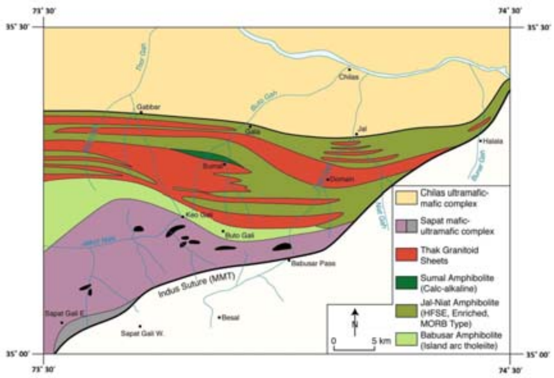

Fig. 2. Geological map of Kamila Amphibolites Unit (after [24])

2. Lithology and Mineralogy of Kamila amphibolites

The Kamila amphibolites are comprised of metavolcanics of crustal sequence [11]. These are metamorphosed to epidote amphibolites due to the intrusion of granitoids of the Thak complex within metavolcanics and the Chilas complex in the north. Some amphibolites also contain traces of garnets [10, 17, 18]. The Kamila amphibolites are fine to coarse grained but generally appear as medium grained. Amphibolites are generally well foliated and banded [5, 8, 10]. These rocks are generally medium grained, hypidioblastic to xenoblastic and porphyroblastic at places, and mainly composed of amphibole (hornblende and actinolite), plagioclase and/or epidote, chlorite, and/or quartz with some garnet at places. Sphene, magnetite, muscovite and apatite are the accessory minerals [5, 10]. On the basis of variation in texture and mineral content, these amphibolites are further subdivided into four distinct groups as mentioned above [3, 10, 11].

2.1. Niat amphibolites

The NW trending Niat rocks are composed of a 50 to 100 m thick belt of fine grained, strongly foliated amphibolites that extends from east to west in the central part of the study area. The Niat amphibolites are bounded on the north by diorites and granodiorites and on the south by diorites of the Thak complex. A tectonic slice of about 500 m of Sumal amphibolites is exposed in the Keo and Buto valleys within it. Westward the belt gradationally merges with the Babusar amphibolites, whereas eastward it is truncated by the MMT. Amphibolites are strongly deformed and appear dark green due to retrogression to chlorite along the foliation. Laminated appearance is also due to the presence of levels rich in quartz. Amphibolites are generally intruded by diorites, granodiorites and tonalities. Some relict pillows are so strongly sheared that their cores and crusts give the impression of banded amphibolites, similar to those of central Kohistan to the south of Jaglot [23]. These pillows are generally composed of light green epidote-chlorite rich cores with dark crust.

2.1.1. Petrography

The Niat amphibolites are fine to medium-grained and occur as alternating mafic and felsic bands. Felsic bands are not foliated in some rocks. Amphibole (64% to 84%) and substantial quartz (8% to 26%) are the dominant constituents of Niat rocks with subordinate plagioclase, epidote and chlorite (Table 1). Magnetite, sphene, muscovite, and apatite occur as accessory minerals. Amphibole (hornblende and actinolite) is sub idiomorphic, green (pleochroic sometimes to bluish green), and ranges from 64% to 85%. Hornblende shows perfect cleavage and sharp boundaries with epidote and quartz, with altered margins. Actinolite is strongly foliated and associated with epidote and chlorite. Plagioclase is sub idiomorphic to idiomorphic and ranges from traces to 7%; it is highly saussuritized and cloudy, and does not show twinning. Two types of plagioclase have been observed; the large crystals have higher anorthite content (andesine An38-44) and the small crystals are albitic (An6-10). The margins are corroded and cores are sericitised, usually enclosed by quartz and some epidote. Sphene is irregularly distributed and occurs as small independent grains or in granular aggregates. Chlorite occurs as flaky aggregates. Opaque oxides are sparsely spread. Quartz is present in alternating bands with the deformed bands of mafic minerals such as amphiboles.

Table 1. Modal composition (Vol.% on visual estimates) of Niat amphibolites

Sample No.	A-82	A-89	A-114	A-200	A-221	A-132	A-134	A-135
Amphibole	84	76	85	78	84	64	70	74
Plagioclase	tr			2		3	4	7
Epidot	1	6	3	1	2	5	3	2
Quartz	15	16	11	14	8	26	16	13
Chlorite				3	4		6	3
Magnetite		2				tr	tr	tr
Sphene	tr	tr	1	tr	1	1	tr	
Biotite								
Calcite								
Muscovite			tr	1	1	1	1	1
Apatite								tr
	100	100	100	99	100	100	100	100

2.2. Jal amphibolites

The Jal amphibolites are well exposed in the Thak and Niat valleys with a width of about 3 km. The Jal amphibolites are bounded by the Chilas complex in the north and diorites of the Thak complex in the south. The contact with the Chilas complex is marked by strongly sheared amphibolite and a granite mylonite zone along Jal shear zone [16, 26]. Towards the east, in Buner valley the rocks are in direct contact with the MMT. The Jal amphibolites are generally fine-grained, melanocratic, banded and foliated. Bands are marked by the enrichment of mafic and felsic material. They are generally dark green, especially along schistosity planes.These planes are marked by the growth of randomly oriented crystals of acicular hornblende. White to light grey granite pegmatites and quartzofeldspathic veins are abundantly intruded into the amphibolites. The granite pegmatite bodies are folded and boudinaged. Ptygmatic folding is the most prominent feature of these rocks. At places, the two rock-types (quartzofeldspathic bodies and amphibolites) show a great degree of mixing.

2.2.1. Petrography

The Jal rocks are mainly medium to coarse-grained and are strongly mylonitized and foliated in E-W direction. Amphibole, chlorite and magnetite are concentrated in the mafic bands while the felsic bands are enriched in plagioclase, quartz and some epidote. Sphene, when present, tends to be concentrated in the mafic bands. Twin planes, cleavage traces and crystal faces are bent and kinked at many places.

Hornblende is the dominant mineral in the rock and ranges from 9% to 76 vol% (Table 2). It is medium-grained, brown green to dark green and shows perfect cleavage. Some crystals show inclusions of quartz and sericite. Along the margins, where hornblende is in contact with plagioclase crystals, a rim of epidote and sphene is present. Magnetite is also present along the boundaries of hornblende. Plagioclase is medium-grained and xenoblastic. Its proportion ranges from 14 to 49 vol%. Its composition ranges from oligoclase through andesine (An30-46) to labradorite (An56), but mostly is in the andesine range. A few samples contain minor microcline. Plagioclase is highly saussuritized, especially the more calcic type (An42-56). The andesine with low anorthite content (An30-42) is less saussuritized. Myrmekitic intergrowth is present in some samples. Quartz is fine to medium-grained and anhedral. Its grains are interfingered with hornblende and plagioclase and forming notched boundaries.

3. Whole Rock Geochemistry

Twenty six rock samples from the Niat and Jal amphibolites have been analyzed for whole-rock geochemistry (Tables 3 & 4) by using Shimadzu (VF-310 model) X-Ray Fluorescence Spectrometer at National Centre for Excellence in Geology, University of Peshawar, Peshawar, Pakistan. Samples were also analyzed at the University of Oklahoma, Norman, USA. The analyses were performed only on homogeneous samples devoid of low-temperature alteration.

Table 2. Modal composition (Vol.% on visual estimates) of Jal amphibolites

Sample No.	A-76	A-156	A-158	A-159	A-69	A-148	A-151	A-89
Amphibole	65	46	54	51	60	76	30	9
Plagioclase	14	17	28	29			49	40
Epidot	3	3	2	2	15	1	6	5
Quartz	16	9	12	13		18	9	5
Chlorite		23			17	4		26
Magnetite		tr	tr	tr	2		5	2
Sphene	1	1	1	1	1	1		
Biotite	1				5			
Calcite								12
Muscovite		1	3	4			1	1
Zircon		tr		tr				
	100	100	100	100	100	100	100	100

Table 3. Major (wt %) and trace element (ppm) data of Niat amphibolites

Sample Nos.	A-80	A-83	A86	A-92	A-93	A-109	A-112	A-114	A-115	A-116	A-132	A-133	A-135
SiO2	50.25	51.19	47.98	49.21	48.76	46.71	48.37	46.59	51.58	48.49	55.56	52.09	44.94
TiO2	2.13	2.24	2.13	1.72	1.86	1.74	2.52	1.73	2.38	1.2	1.91	1.75	2.58
Al2O3	14.75	14.31	14.44	15.23	14.71	15.11	17.96	15.21	14.24	15.75	15.4	14.82	13.04
Fe2O3	14.67	14.67	14.08	11.91	13.06	12.55	14.3	12.45	13.63	10.41	11.76	12.52	15.93
MgO	6.32	5.11	6.11	6.51	6.9	8.38	2.69	8.43	4.65	11.61	4.03	5.76	7.6
CaO	8.33	9.63	11.64	12.39	11.82	12.98	8.35	12.95	10.43	10.2	7.18	8.55	13.05
Na2O	3.11	2.4	3.09	2.73	2.66	2.25	5.18	2.36	2.68	2.19	3.74	4.14	2.56
K2O	0.23	0.26	0.32	0.14	0.08	0.09	0.06	0.08	0.2	0.06	0.08	0.16	0.09
P2O5	0.21	0.19	0.21	0.16	0.17	0.19	0.58	0.2	0.21	0.09	0.34	0.21	0.22
Total	100	100	100	100	100.02	100	100.01	100	100	100	100	100	100.01
Nb	5.2	4.8	6.2	4.1	4.3	0.9	1.6	4.9	4.6	2.1	19	7.8	5.2
Zr	150	139	149	113	114	25	6	134	140	79	142	203	63
Y	57	53	52	37	40	21	37	55	49	26	98	57	47
Sr	172	150	137	165	169	193	247	183	138	175	146	132	114
Rb	1	2	2	1	1	1	1	1	1	1	1	1	1
Th	2	2	2	2	2	2	2	2	2	2	2	2	2
Pb	2	2	2	2	2	2	2	2	2	2	2	2	2
Ga	24	22	23	18	20	17	32	22	22	15	23	23	23
Zn	110	93	101	70	78	63	102	15	25	71	107	106	119
Cu	8	14	12	78	15	13	43	2	2	67	23	67	101
Co	51	54	54	60	60	58	48	43	53	55	57	61	66

Table 3. (Continued)

Ni	32	22	75	67	58	136	8	22	22	25	34	57	73
Ti	12769.5	13429	12769.56	10311.57	11150.89	10431.47	15107.65	10371.52	14268.3	7194.12	11450.64	10491.4	15467.36
K	1909.37	2158.42	2656.51	1162.22	664.13	747.14	498.1	664.13	1660.32	498.1	664.13	1328.26	747.14
P	916.52	829.24	916.52	698.3	741.95	829.24	2531.35	872.88	916.52	392.8	1483.9	916.52	960.17
Mg	38116.55	30818.92	36850.02	39262.46	41614.59	50540.62	16223.66	50842.17	28044.62	70021.07	24305.33	34739.14	45836.36

Table4. Major (wt %) and trace element (ppm) data of Jal amphibolites

Sample Nos.	A-69	A-72	A-78	A-74	A-98	A-101	A-105	A-147	A-148	A-151	A-154	A-156	A-157
SiO2	49.33	50.13	51.89	50.19	50.11	50.72	51.79	49.08	49.42	54.77	50.17	51.9	48.9
TiO2	1.13	1.64	0.73	1.52	2.91	1.15	2.39	1.15	2.03	0.54	2.13	1.93	1.1
Al2O3	16.74	14.68	20.19	14.55	13.4	15.49	13.89	15.41	14.25	18.27	13.99	15	16.06
Fe2O3	9.65	11.87	9.25	12.19	16.42	11.14	14.61	11.57	13.34	8.62	13.43	12.91	9.83
MgO	9	7.3	4.86	6.81	5.63	7.69	5.65	8.55	6.64	4.47	6.31	6.54	9.24
CaO	11.57	11.34	9.52	11.68	7.61	11.83	8.49	12.16	11.29	9.99	9.96	9.49	11.58
Na2O	2.34	2.76	3.32	2.69	3.44	1.7	2.85	1.54	2.52	2.87	3.56	1.97	2.88
K2O	0.14	0.13	0.17	0.23	0.13	0.15	0.08	0.45	0.3	0.32	0.24	0.07	0.32
P2O5	0.1	0.15	0.06	0.13	0.35	0.12	0.25	0.09	0.2	0.15	0.21	0.18	0.1
Total	100	100	99.99	99.99	100	99.99	100	100	99.99	100	100	99.99	100.01
Nb	2.8	3.1	0.7	3.1	8	3.1	6.5	3	5.4	2.1	5.6	5	2.6
Zr	68	85	20	85	168	64	160	76	126	51	135	118	66
Y	22	34	11	34	59	28	50	28	43	17	45	40	22
Sr	164	185	475	185	162	176	144	173	153	250	128	227	158
Rb	1	1	1	1	1	2	1	15	4	1	2	1	3
Th	2	2	2	2	2	2	2	2	2	3	2	2	2
Pb	2	2	2	2	2	2	2	2	2	4	2	2	2
Ga	16	20	20	20	22	19	23	19	21	18	21	19	16
Zn	64	99	78	99	210	119	180	104	95	80	98	98	68
Cu	5	18	28	18	814	76	179	2	54	47	33	23	2
Co	57	59	54	59	50	69	49	67	54	36	52	56	61
Ni	129	50	7	50	25	94	33	97	64	17	40	42	154
Ti	6774.46	9831.96	4376.42	9112.55	17445.74	6894.37	14328.29	6894.37	12170.05	3237.35	12769.56	11570.54	6594.61
K	1162.22	1079.21	1411.27	1909.37	1079.21	1245.24	664.13	3735.72	2490.48	2656.51	1992.38	581.11	2656.51
P	436.44	654.66	261.86	567.37	1527.54	523.73	1091.1	392.8	872.88	654.66	916.52	785.59	436.44
Mg	54279.9	44027.03	29311.15	41071.79	33955.09	46379.16	34075.72	51565.91	40046.5	26959.02	38056.24	39443.39	55727.36

3.1. Major Element Geochemistry

Jal and Niat amphibolites are classified as basalts and basaltic andesites on the SiO2 –(Na2O+K2O) plot of [27]. One sample plot is in the field of trachybasalt (Fig. 3). On the R1-R2 classification scheme of [28, 29] the majority of them fall in the basalt field with some plotting in the field of andesite-basalt, and a few in the andesite field. The majority of amphibolites are tholeiitic in nature on FeOt/MgO-SiO2 plot of [30] with a few plotted on the calc-alkaline field (Fig. 4). AFM diagram of [31] also confirmed the tholeiitic trend (Fig. 5).

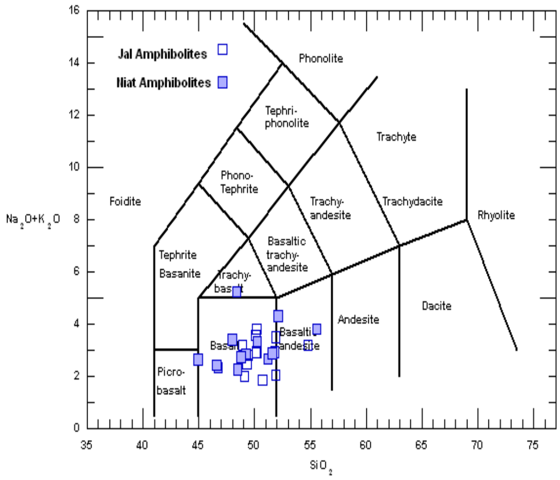

Fig. 3. The chemical classification and nomenclature of studied rock using the total alkalis versus SiO2 (TAS) Plot (after [27])

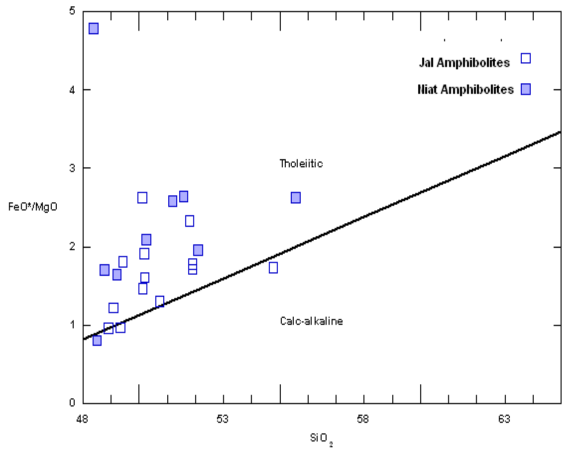

Fig. 4. Bivariate plot of FeO*/MgO versus SiO2 showing the tholeiitic nature (after [30])

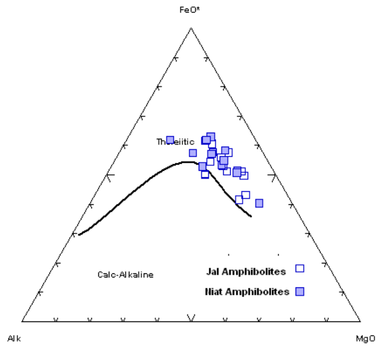

Fig. 5. AFM diagram with boundary between tholeiite and calc-alkaline rocks (after [31]), most of Jal and Niat rocks plot in tholeiite field

3.1.1. Fractionation Assemblage

Depletion of MgO (Fig. 6) with advancing fractionation (using Zr as a fractionation index), is indicative of early crystallization of olivine and/or pyroxene in the Jal-Niat rocks. Fe2O3 and TiO2 show a good mutual correlation and enrichment with increasing proportions of Zr (Fig. 6), suggesting a lack of crystallization of iron-rich minerals such as magnetite and ilmenite. CaO shows a near constant trend with increasing fractionation while Al2O3 shows a remarked depletion, suggesting the crystallization of spinels in earlier stages of fractionation followed by the Ca depleted plagioclase and clinopyroxene in later phases. Iron enrichment trend together with crystallization of plagioclase in the fractionation history are typical features of MORB tholeiites [32].

3.2. Trace Element Geochemistry

The Jal and Niat amphibolites are generally poor in large ion lithophile elements (LILE) such as Rb, Pb, Th and K. Sr concentration is controlled by the fractionation of plagioclase in the initial stages, and by both plagioclase and clinopyroxene in the later stages. This is shown by its inversely proportional relationship against Zr. Amongst the high-field strength elements (HFSE) Ti concentration is controlled by a lack of crystallization of a Ti phase in tholeiites of the studied site. Other HFSE like Zr, Y, and P are truly incompatible and suitable for use in petrogenesis of the studied Jal-Niat rocks. Their concentrations are about ten times higher than those in chondrites.

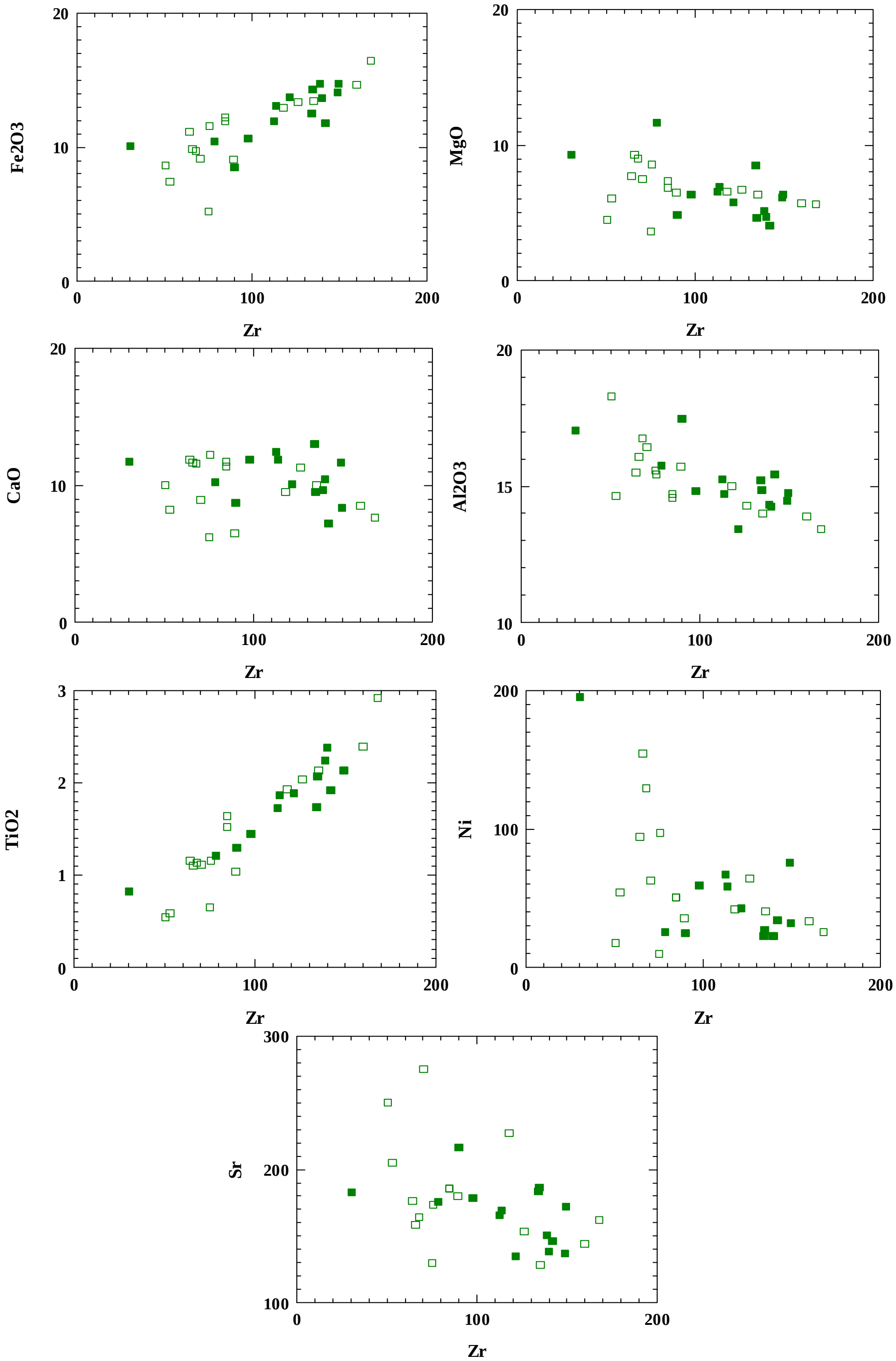

Fig. 6. Binary plots of different oxides and trace elements versus Zr

3.2.1. Ferromagnesian Elements

Crystal-liquid distribution coefficient data indicate that Ni and Co will partition into olivine during partial melting and fractional crystallization processes, while Sr, Cr and V will enter clinopyroxene. Thus knowledge about the amounts of these elements should be useful in studying petrogenetic processes [32-36]. Ni abundances in MORB are strongly controlled by olivine fractionation [32]. Ni ranges from >300 ppm in primitive glassy basalts to 25 ppm in highly evolved basalts and correlates well with MgO content. In the studied rocks Ni ranges from >150 to <10 (Table 5). This shows the middle character of the rocks, which are neither highly evolved nor primitive. When plotted against Zr, elements like Ni and Sr display decrease in concentration with increasing contents of Zr. This decrease with increasing Zr abundance implies that much of the chemical variation in these rocks may be attributed to crystal fractionation processes.

Table5. Average major(wt %) and trace element (ppm) composition of primitive samples from Jal-Niat amphibolites and their comparison with various tectonic settings

Sample	JAL	NIAT	N-MORB	P-MORB	IAT	BAT	OIT
SiO2	50.64	49.36	50.55	49.72	49.2	50.36	50.51
TiO2	1.56	1.99	1.27	1	0.52	1.46	2.63
Al2O3	15.53	14.99	16.38	15.81	15.3	16.36	13.45
Fe2O3	11.91	13.22	1.27	1.66		9.07	1.78
MgO	6.82	6.46	7.8	7.9	10.1	7.36	7.41
CaO	10.5	10.57	11.62	11.84	13	10.84	11.18
Na2O	2.64	3	2.79	2.35	1.51	3.39	2.28
K2O	0.2	0.14	0.07	0.25	0.17	0.43	0.49
P2O5	0.16	0.22	0.12	0.14	0.06	0.2	0.28
Total	99.96	99.95					
Nb	3.92	5.44	2.33	8.33	0.7	8	17
Zr	94	112	74	73	22	130	115
Y	33.3	48.38	28	22	12	30	25
Sr	198.46	163	90	155	200	212	371
Rb	2.61	1.15	0.56	5.04	4.6	6	9.2
Th	2	2	0.12	0.6	0.25		1.64
Pb	2	2	0.3				5
Ga	19.53	21.84				15	
Zn	107	81.53				68	
Cu	99.92	34.23					
Co	55.61	55.38					
Ni	61.69	48.54	138	32		64	
Ti	9352.36	11930.25	7607.78	6007.09	3117.45	8752.85	15767.11
K	1660.32	1162.22	597.72	2092	1411.27	3569.69	4067.78
P	698.3	960.17	510.63	624.11	261.86	872.88	1222.03

Table 5. (Continued)

Mg	41132.1	38960.91	47042.58	47645.69	60914.11	44388.9	44690.45
Sr/Rb	76.03	141.73	160.71	30.75	43.47	35.33	40.32
K/Rb	633.7	1010.62	1067.35	415.07	306.79	594.94	442.15
Ti/Zr	99.49	106.52	102.81	82.29	141.7	67.33	137.11
Zr/Y	2.82	2.32	2.64	3.32	1.83	4.33	4.6
Zr/P2O5	587.5	509.09	632.48	510.49	366.67	650	410.71

Sources of data: N-MORB and P-MORB [52]; IAT [37]; BAT [42]; OIT [38]. The total is not 100% here because some oxides are excluded

3.2.2. Inter-element Ratios

Ratios between truly incompatible trace elements are of great significance in petrogenetic studies. They provide a tool to see through the effects of processes like fractional crystallization and partial melting, and reflect the composition of not only the parent melt but also that of the source [33].The element ratios K/Rb (i.e. 633 for Jal amphibolites and 1010 for Niat amphibolites) and Sr/Rb (i.e. 76 for Jal amphibolites and 141 for Niat amphibolites) are characteristically higher for these amphibolites and are similar to MORB (Table 5). Zr abundances range from 20 to 203 ppm with an average of 94 and 112 ppm for Jal and Niat amphibolites respectively. There are good collinear trends between Zr and Ti, Y, and P, and the average ratios of Ti/Zr, Zr/Y and Zr/ P_2O_5 for Jal and Nait Amphibolites are 99, 2.5 and 548 respectively, which are very close to those of N-MORB (Table 5).

3.2.3. Trace-element Patterns as Spidergrams

Trace-element patterns for four samples from the studied suite of Jal and Niat amphibolites, covering the range from the most primitive through intermediate to the most evolved compositions are presented in (Figs. 7 & 8) [37, 38]. The concentration of incompatible trace elements like Zr, Y, P and Nb are progressively increasing from the most primitive composition (A-69, A-157) to most evolved composition (A-86, A-105). In the most evolved sample, it is 20 times the primordial mantle. The identical patterns of these four samples suggest a close petrogenetic relationship and a common source.Conventional spidergrams [35] include a greater number of trace elements including Rb, K, Sr and Ti, which, though incompatible with respect to the mantle mineralogy, behave compatibly during fractional crystallization. The four selected samples, when plotted on such a spidergram (Fig. 7) do not show matching shapes for the patterns. For instance, Ti is low in primitive compositions but shows higher concentrations in the evolved samples. This is probably a reflection of the iron-enrichment trend as deduced from the major-element variations. Sr shows the opposite relationship shown by Ti. Primitive samples have high Sr while the evolved ones are marked with a negative Sr anomaly, reflecting the role of plagioclase fractionation.

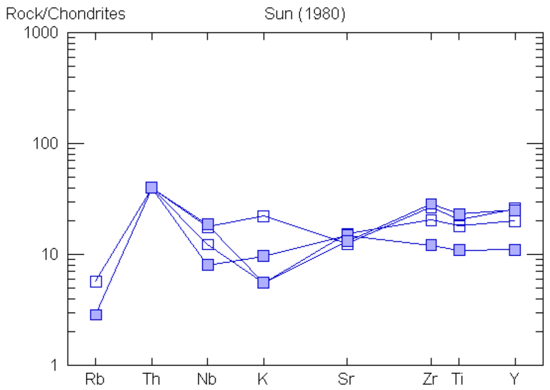

Fig. 7. Rock/Primitive Mantle diagram of Niat-Jal amphibolites (after [37])

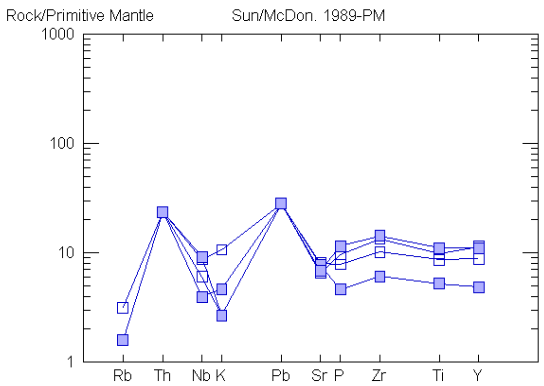

Fig. 8. Rock/Primitive Mantle diagram of Niat-Jal amphibolites (after [38])

4. Petrogenesis

The chemistry of the rocks shows intermediate characteristics between N-type and P-type MORB. For instance, Zr/Nb ratios (mean= 24 and 21 for Jal and Niat amphibolites, respectively) have transitional behavior because N-MORB has high ratios (>30) whereas P-MORB has low ratios (<10). Trace element patterns (Figs. 7 & 8) suggest these rocks were unaffected by subduction [39]. Since the shape of these patterns is little affected by differences in partial melting and fractional crystallization histories [34], the variations between the patterns are best explained in terms of heterogeneities in mantle source [39]. The geochemical patterns of rocks are similar to the tholeiites but enriched in Nb, Zr, Sr, Rb, Th and Pb elements. This enrichment may possibly be due to contamination or mixing of a more depleted source by enriched mantle.

K and Rb show high concentrations in primitive samples whereas the evolved ones having low concentrations like Sr but a combination of factors (low concentrations either below or only marginally above the detection limit of the analyzing instrument, and possibility of remobilization during metamorphism) cause discrepancies in their ratios relative to HFS elements. However, when the elements (Rb, K and Sr) with very low concentrations or suspected of remobilization are excluded, the four selected samples have mutually similar trace elements patterns suggesting cogenetic origin (Figs. 7 & 8).

The enhanced LILE / HFSE ratios in the rocks may be due to incorporation of slab derived material within the depleted mantle source [e.g. 32, 40-48]. This feature results in selective enrichment in certain elements (Rb, Ba, K, Sr, +Ce+Sm+P) and a relative lack of enrichment in others (Nb, Zr, Ti, Y) [39]. Table 5 shows selected trace element ratios of the studied rocks compared with the mid ocean ridge basalt (MORB), island arc tholeiites (IAT), and oceanic island tholeiites (OIT). The studied rocks show resemblance with the N type MORB. However, the enrichment in HFS elements indicates that they are developed from a more heterogeneous and enriched mantle than a typical MORB like source.

5. Tectonic Environment

The majority of the studied samples have concentration of TiO_2 (1-3 wt%; mean=1.56 wt% Jal Amphibolites; 1.99 wt% Niat Amphibolites) and K_2O (mean=0.2 wt% Jal Amphibolites; 0.14 wt% Niat Amphibolites) similar to MORB as [49]. [50] reported that the Y/Nb ratio is constant during metamorphism and alteration. The average Y/Nb ratio for Jal and Niat is 8.4 and 8.9, respectively, which is close to N-MORB (i.e. 12) and much higher than P-MORB (2.64) (Table 5). The rocks show a closer correspondence to the MORB (mid-ocean ridge basalts) than the IAT (island arc tholeiites) or CAB (calc alkaline basalts). Various established discrimination diagrams have been applied to the studied rocks to know their magmatic affinity and tectonic environment. In the majority of cases the rocks plot in the field of ocean floor basalts as on Ti/100, Zr and Y*3 and Ti/100, Zr and Sr/2 plots of [51] (Figs. 9 & 10). A plot of Zr/Y vs Zr [41] discriminates effectively between basalts from ocean island arcs, MORB and within plate environments (Fig. 11). This plot can also be used to subdivide island-arc basalts into those belonging to oceanic arcs, where only oceanic crust is used in arc construction, and arcs developed at active continental margins. All the samples plot in the field of MORB. [52] Suggesting that the immobile trace element Nb could be used to separate the different types of ocean-floor basalt. A triangular plot of Zr/4, 2 x Nb and Y displays the rocks of the study area in the field of N-type MORB (Fig. 12). From these discriminate diagrams, it is concluded that the Jal-Niat amphibolites of the study area are essentially tholeiitic in nature and developed in mid-ocean ridge setting.

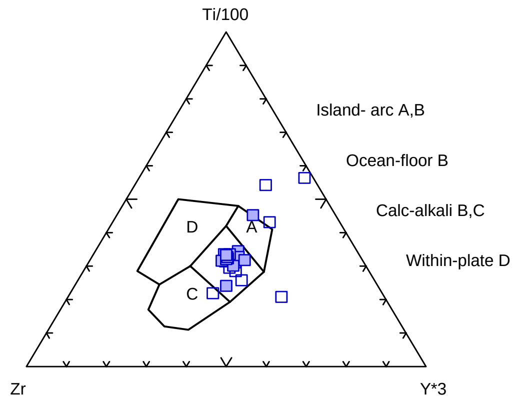

Fig. 9. Ti/100, Zr and Y*3 Plot of Niat-Jal amphibolites (after [51])

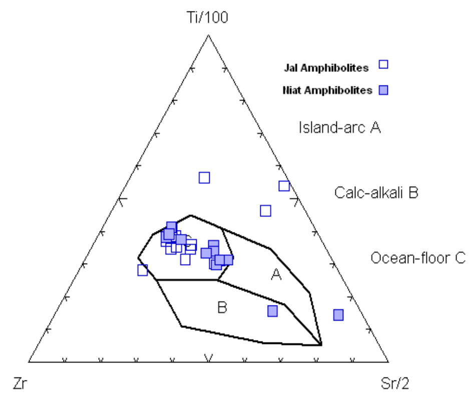

Fig. 10. Ti/100, Zr and Sr/2 Plot of Niat-Jal amphibolites (after [51])

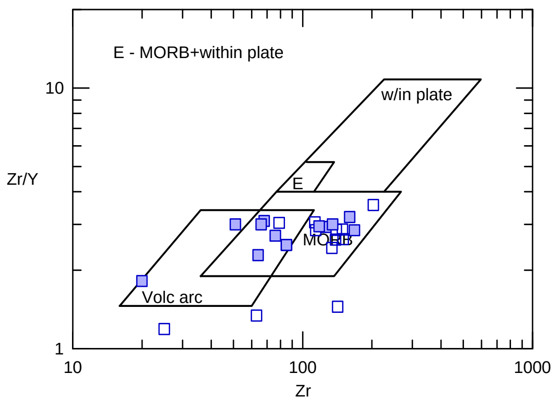

Fig. 11. Zr/Y versus Zr Plot of Niat-Jal amphibolites (after [41])

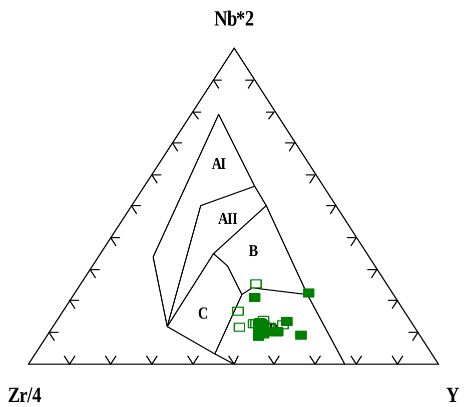

Fig. 12. Nb*2, Zr/4 and Y Plot of Niat-Jal amphibolites (after [52]), where AI (Within plate Basalts), AII (Within plate Basalts and Within Plate Tholiites), B (E-MORB), C (Within Plate Tholiites and Volcanic Arc Basalts) and D (N-MORB)

6. Discussion and conclusion

Petrographically, Niat and Jal amphiboltes can easily be distinguished on the basis of variation in texture and mineral content. Niat amphibolites are fine to medium grained and composed of hornblende and substantial quartz with subordinate plagioclase, epidote and chlorite. Jal amphibolites are medium to coarse grained and composed of hornblende and plagioclase with some inclusions of quartz and sericite at places. Magnetite, sphene, apatite and muscovite occur as accessory minerals in both groups.

The geochemical data clearly reveals that Niat and Jal amphibolites are tholeiitic basalts of ocean floor, developed in mid-oceanic ridge settings. Trace element ratios suggest that Niat and Jal amphibolites were unaffected by subduction zone fluids and magmas. The studied rocks show close resemblance with N-type MORB but are enriched in Nb, Zr, Sr, Rb, Th and Pb elements which enhanced the LILE / HFSE ratios. This enrichment is possibly caused by the incorporation of slab derived material within the depleted mantle source.

References

[1] Bignold, S. M. & Treloar, P. J. (2003). Northward subduction of the Indian Plate beneath the Kohistan island arc, Pakistan Himalaya: new evidence from isotopic data. Jour. *Geol. Soc. London, 160(3)*, 377-384.

[2] Kazmi, A. H. & Rana, R. A. (1982). *Tectonic map of Pakistan*. Quetta, Pakistan: Geol. Surv. Pakistan.

[3] Khan, M. A., Rehman, S., Mehmood, K., Khan, M. A. & Ahsan, N. (2011). Geochemistry, Petrogenesis and Tectonic Environment of Niat-Jal amphibolites, southeast Kohistan, Pakistan. Presented at *26th Himalaya-Karakoram-Tibet Workshop* on July 12-13, 2011, Canmore, Canada.

[4] Tahirkheli, R.A.K., Mattauer, M., Proust, F. & Taponier, P. (1979). The India-Eurasia suture zone in northern Pakistan: Synthesis and interpretation of recent data at plate scale. In: Farah, A., Dejong, K. A., (Eds), *Geodynamics of Pakistan*, Geological Survey of Pakistan, 125-130.

[5] Jan, M. Q. (1979). Petrography of the amphibolites of Swat and Kohistan. *Geol. Bull. Peshawar Univ., 11*, 51-64.

[6] Chaudhry. M. N. & Chaudhry, A. G. (1974). Geology of Khagram area, Dir district. *Geol. Bull. Punjab Univ., 11*, 21-43.

[7] Shams, F. A. (1975). The petrology of the Thak Valley Igneous Complex, Gilgit Agency, North Pakistan. *Rend. Accad. Naz. Lincie, Ser. VIII*, Rome, 453-464.

[8] Ahmed, Z. & Chaudhry, M. N. (1976). Petrology of the Babusar area, Diamir district, Gilgit, Pakistan. *Geological Bulletin, Punjab University, 12*, 67-78.

[9] Misch, P. (1949). Metasomatic granitization of batholithic dimensions, Part I: syntectonic granitization in Nanga Parbat area, North West Himalaya. *American Journal of Science, 247*, 209-245.

[10] Khan, M. A. (1997). Geology of southeast Kohistan, NW Himalayas, Pakistan. Ph.D Thesis, Peshawar University.

[11] Khan, M. A., Rehman, S., Ahsan, N. & Ullah, F. (2009). Geochemistry and tectonic environment of Babusar amphibolites, southeast Kohistan, Pakistan. *Geol. Bull. Punjab Univ., 44*, 105-116.

[12] Martin, N. R., Siddiqui, S. F. A. & King, B. H. (1962). A geological reconnaissance of the region between the lower Swat and Indus rivers of Pakistan. *Geol. Bull. Punjab Univ., 2*, 1-13.

[13] Davies, R. G. (1965). The nature of the Upper Swat Hornblendic Group of Martin et al. (1962). , *Geol. Bull. Punjab Univ 2*, 51-52.

[14] Jan, M. Q. & Kempe, D. R. C. (1973). The petrology of basic and intermediate rocks of upper Swat, Pakistan. *Geol. Mag., 110*, 285-300.

[15] Tahirkheli, R. A. K. & Jan, M. Q. (1979). A preliminary geological map of Kohistan and the adjoining areas, N. Pakistan. Geol. Bull., Peshawar Univ., 11 (Special Issue), (in pocket).

[16] Coward, M. P., Windley, B. F., Broughton, R. D., Luff, I. W., Petterson, M. G., Pudsey, C. J., Rex, D. C. & Khan, M. A. (1986). Collision tectonics in the NW Himalayas. In: Coward, M.P. and Ries, A.C. (eds.) Collision Tectonics. *Geological Society of London, Special Publication, 19*, 203-219.

[17] Jan, M. Q. (1988). Geochemistry of amphibolites from the southern part of the Kohistan arc, N. Pakistan. *Mineralogical Magazine, 52*, 147-159.
[18] Bard, J.P., Maluski, H., Matte, Ph. & Proust, F. (1980). The Kohistan sequence; Crust and mantle of an obducted island arc. *Geol. Bull. Peshawar Univ., 13*, 87-93.
[19] Bard, J.P. (1983a). Metamorphism of an obducted island arc: Example of the Kohistan sequence (Pakistan) in the Himalayan collided range. *Earth and Planetary Science Letters, 65*, 133-144.
[20] Bard, J.P. (1983b). Metamorphic evolution of an obducted island arc: Examples of the Kohistan sequence (Pakistan) in the Himalayan collided range. *Geol. Bull. Peshawar Univ., 16,* 105-184.
[21] Jan, M. Q. (1977). The Kohistan basic complex, a summary based on recent petrological research. *Geol. Bull. Univ. Peshawar,Vol. 9-10,* 36-42.
[22] Jan, M. Q., Khan, M. A. & Qazi, M. S. (1993). The Sapat mafic-ultramafic complex, Kohistan arc, North Pakistan. In: Treloar, P. J. and Searle, M. P. (eds.) Himalayan Tectonics. *Geological Society of London, Special Publication, 74,* 113-121.
[23] Khan, T., Khan, M. A. & Jan, M. Q. (1994). Geology of a part of the Kohistan terrane between Gilgit and Chilas, northern areas, Pakistan. *Geol. Bull. Peshawar Univ., 27*, 99-112.
[24] Khan, M. A, Khan, M. A. & Jan, M. Q. (1997). Geology of southeast Kohistan, Northwest Himalaya, Pakistan. *Jour. Nepal Geol. Soc., 1997, 16, (Sp. Issue)*
[25] Khan, M. A. & Qazi, M. S. (2005). Multiple sources of magmatism: granitoid from southeast Kohistan, NW Himalaya, Pakistan. *Geol. Bull. Univ. Peshawar, Vol. 38*, 89-112.
[26] Khan, M. A. (1988). Petrology and Structure of the Chilas Ultramafic-Mafic Complex, N. Pakistan. Ph.D. thesis, University of London*.*
[27] Le Maitre, R. W., Bateman, P., Dudek, A., Keller, J., Lameyre, Le Bas, M. J., Sabine, P. A., Schmid, R., Sorensen, H., Streckeisen, A., Woolley, A. R. & Zanettin, B. (1989). A classification of igneous rocks and glossary of terms. *Blackwell, Oxford.*
[28] De la Roche, H., Leterrier, J., Grande, Claude, P. & Marchal M. (1980). A classification of volcanic and plutonic rocks using R1-R2 diagrams and major element analyses - its relationships and current nomenclature. *Chemical Geology, 29*, 183-210.
[29] Jensen, L. S. (1976). A new cation plot for classifying subalkalic volcanic rocks. Ontario Division Mines. *Misc. Pap., 66*.
[30] Miyashiro, A. (1974).Volcanic rock series in island arcs and active continental margins. *American Journal of Science 274*, 321-355.
[31] Irvine, T. N. & Barager, W. R. A. (1971). A guide to the chemical classification of the common volcanic rocks. *Canadian Journal of Earth Sciences, 8,* 523-548.
[32] Wilson, M. (1989). Igneous petrogenesis, a global tectonic approach. *Unwin Hyman, London.*
[33] Weaver, B. L., Tarney, J. & Windley, B. (1981). Geochemistry and petrogenesis of the Fiskenaesset anorthosite complex southern West Greenland: nature of the parent magma. *Geochemic & Cosmochimic Acta, 45*, 711-725.
[34] Pearce, J. A. (1983). Role of the sub-continental lithosphere in magma genesis at active continental margins. In: Hawkesworth, C. J. & Norry, M. J. (eds.) Continental Basalts and Mantle Xenoliths. *Shiva Publishing, Nantwich,* 230-249.
[35] Thompson, G., Bryan, W. B. & Melson, W. G. (1980). Geological and geophysical investigation of the Mid-Cayman Rise spreading center: geochemical variation and petrogenesis of basalt glasses. *Journal of Geology, 88*, 41-55.
[36] O'Donnell, T. H. & Presnall, D. C. (1980). Chemical variation of the glass and mineral phases in basalts dredged from 250 - 300 N along the Mid-Atlantic Ridge. *Ameri. Jour. Science, 280A*, 845-868.
[37] Sun, S.-S. (1980). Lead isotopic study of young wlcanogenic rocks from mid-ocean ridges, ocean islands and island arcs. *Philosophical Transactions of the Royal Society of London, A297*, 409-445.
[38] Sun, S.-S. & Mcdonough, W.F. (1989). Chemical and isotopic systematics of oceanic basalts: implications for mantle composition and processes. In: Saunders, A.D. & Norry, M.J. (eds) Magmatism in the Ocean Basins. *Geol. Soc. London, Special Publications, 42*, 313-345.
[39] Pearce, J. A., Harris, N. B. W. & Tindle, A. G. (1984). Trace element discrimination diagrams for the tectonic interpretation of Granitic rocks. *Journal of Petrology, 25*, 956-983.
[40] Hawksworth, C. J., O'Nions, R. K., Himilton, P. J. & Evensen, N. M. (1977). A geochemical study of island arc and back-arc tholeiites from the Scotia Sea. *EPSL, 36*, 253-262.
[41] Pearce, J. A. & Norry, M. J. (1979). Petrogenetic implications of Ti, Zr, Y and Nb variations in volcanic rocks. *Contributions to Mineralogy and Petrology, 69*, 33-47.
[42] Saunder, A. D. & Tarney, J. (1979). The geochemistry of basalts from a back-arc spreading Centre in the East Scotia Sea. *Geochemic and Cosmochimic Acta, 43*, 555-572.
[43] Saunders, A. D. & Tarney, J. (1991). Back-arc basins. In: Floyd, P. A. (eds.) Oceanic basalts. *Blackie and Nostrand Reihold*, 219-263.
[44] Green, T. H. & Hellman, P. L. (1982). Fe-Mg partitioning between coexisting garnet and phengite at high pressure, and comments on a garnet-phengite barometer. *Lithos, 15*, 253-266.
[45] Wyllie, P. J. (1982). Subduction products according to experimental prediction. *Geol. Soc. America Bulletin, 93*, 468-476.
[46] Wyllie, P. J. (1984). Constraints imposed by experimental petrology on possible and impossible magma sources and products. *Philosophical Transactions of the Royal Society of London, A310*, 439-456.
[47] Arculus, R. J. & Powell, R. (1986). Source component mixing in the regions of arc magma generation. *Journal of Geophysical Research, 91*, 5913-5926.
[48] Woodhead, J. D., Eggins, S. M. & Jonson, R. W. (1998). Magma Genesis in the New Britain Island Arc: Further Insights into Melting and Mass Transfer Processes. *Journal of Petrology, 39*, 1641-1668.
[49] Pearce, J. A. (1976). Statistical analysis of major element patterns in basalts. *Journal of Petrology, 17,* 15-43.
[50] Winchestor, J. A. & Floyd, P. A. (1976). Geochemical magma type discrimination application to altered and metamorphosed basic igneous rocks. *EPSL, 28,* 459-469.

[51] Pearce, J. A. & Cann, J. R. (1973). Tectonic setting of basic volcanic rocks determined using trace element analyses. *EPSL, 19*, 290-300.

[52]. Meschede, M. (1986). A method of discriminating between different types of mid ocean ridge basalts and continental tholeiites with the Nb-Zr-Y diagram. *Chemical Geology, 56*(3-4), 207-218.